PROCEEDINGS OF SCIENCE

Nucleon form factors and structure functions from $N_f = 2$ clover fermions

QCDSF/UKQCD Collaboration: S. Collins,[a] M. Göckeler,[a] Ph. Hägler,[a] T. Hemmert,[a] R. Horsley,[b] Y. Nakamura,[a,c] A. Nobile,[a] H. Perlt,[d] D. Pleiter*,[e] P.E.L. Rakow,[f] A. Schäfer,[a] G. Schierholz,[e] A. Sternbeck,[a] H. Stüben,[g] F. Winter[a] and J.M. Zanotti[b]

[a] *Institut für Theoretische Physik, Universität Regensburg, 93040 Regensburg, Germany*
[b] *School of Physics, University of Edinburgh, Edinburgh EH9 3JZ, UK*
[c] *Center for Computational Sciences, University of Tsukuba, Ibaraki 305-8577, Japan*
[d] *Institut für Theoretische Physik, Universität Leipzig, 04109 Leipzig, Germany*
[e] *Deutsches Elektronen-Synchrotron DESY, 15738 Zeuthen, Germany*
[f] *Theoretical Physics Division, Department of Mathematical Sciences, University of Liverpool, Liverpool L69 3BX, UK*
[g] *Konrad-Zuse-Zentrum für Informationstechnik Berlin, 14195 Berlin, Germany*
Email: dirk.pleiter@desy.de

We give an update on our ongoing efforts to compute the nucleon's form factors and moments of structure functions using $N_f = 2$ flavours of non-perturbatively improved Clover fermions. We focus on new results obtained on gauge configurations where the pseudo-scalar meson mass is in the range of 170-270 MeV. We will compare our results with various estimates obtained from chiral effective theories since we have some overlap with the quark mass region where results from such theories are believed to be applicable.

The XXVIII International Symposium on Lattice Field Theory, Lattice2010
June 14-19, 2010
Villasimius, Italy

*Speaker.

1. Introduction

Over years significant efforts have been made to use lattice techniques to investigate the structure of the nucleon. Of particular interest are the Parton Distribution Functions (PDFs) and form factors. The latter encode information about charge distribution and magnetization while the PDFs tell us about the distribution of momentum and spin. While some of the related observables can be determined with good accuracy by experiments (e.g. the nucleon's axial charge g_{A}) other quantities are difficult to access (like the tensor charge g_{T}).

A precise determination of moments of nucleon PDFs and form factors on the lattice turned out to be rather challenging. It continues to be difficult to reach sufficient control on all systematic errors such as finite size effects, lattice artefacts and the influence of the chiral extrapolation. Simulations are performed in volumes of a size where some quantities exhibit significant finite size effects. The available lattice data of the quantities of interest show no significant discretization effects. But current simulations only probe a small window of lattice spacings thus providing us with limited control on the continuum extrapolation. From chiral effective theories (ChEFT) there are indications that the quark mass dependence close to the physical pion mass is very strong. Therefore extending lattice simulations into the region where $m_\pi \leq m_{\mathrm{PS}} \lesssim 300$ MeV has become a major goal for recent calculations.

2. Simulation details

For our simulations we use Wilson glue and $N_{\mathrm{f}} = 2$ degenerate flavours of Clover fermions, where the improvement coefficient c_{SW} has been determined non-perturbatively. Most of our configurations have been generated using the BQCD implementation of the HMC algorithm [1]. Various algorithmic improvements have been applied which accelerate this algorithm, such as the Hasenbusch preconditioning and the use of multiple time-scales, or reducing the time spent for matrix inversion. For instance, chronological guess and the Schwarz Alternating Procedure (SAP) are used to start the inversion and to precondition the fermion matrix [2].

These algorithmic improvements plus recent increase in computing resources enabled simulations in the region of small quark masses, i.e. in a region where the pseudo-scalar mass is smaller than 300 MeV. Fig. 1a shows the parameter region of our simulations. When approaching physical quark masses larger lattices are needed to stay in the region $m_{\mathrm{PS}}L \gtrsim 3$ where finite size effects are expected to be sufficiently small (see Fig. 1b). To investigate such finite size effects we have also performed simulations with $m_{\mathrm{PS}}L < 3$.

We compute the quark propagators using point sources which we (Jacobi) smear to improve overlap with the ground state. For the three-point correlation functions we apply standard sequential source techniques. The distance between source and sink is about 1 fm. Throughout this paper we will ignore contributions coming from disconnected terms. While these anyhow cancel in the iso-vector cases, results for the iso-scalar case maybe affected by an uncontrolled systematic error.

To set the scale we use the Sommer parameter r_0/a which we extrapolated to the chiral limit at each beta. While on the lattice this quantity can be determined with small statistical errors, there is no experimental determination. We therefore computed the dimensionless quantity $(am_N)(r_0/a)$ on the lattice and use the experimentally well known mass of the nucleon m_N to obtain $r_0 = 0.467\,\mathrm{fm}$.

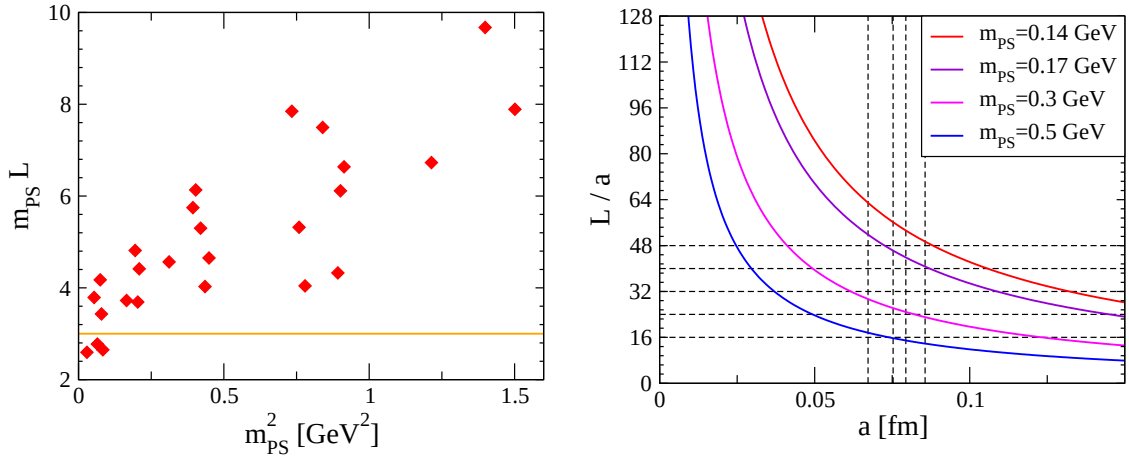

(a) (b)

Figure 1: The left panel shows the simulation points in the $m_{\rm PS}^2$ vs. $m_{\rm PS}L$ plane. In the right panel dashed lines show the lattice spacing and box sizes for which simulations have been performed. In both figures the continuous lines show where $m_{\rm PS}L = 3$.

Most of the quantities considered in this paper need to be renormalised. The renormalisation constants have been determined using the RI$'$−MOM scheme [3], except for the vector current renormalisation constant Z_V. Here we applied the condition that the nucleon's local vector current at zero momentum must be 1. If necessary, the results are converted into $\overline{\rm MS}$ scheme using the 4- and 2-3-loop expressions of the β function and corresponding anomalous dimension γ, respectively.

3. Lowest moments of PDFs

Let us first consider the lowest moment of the polarized nucleon PDF $\langle 1\rangle_{\Delta q}$ (also known as axial coupling constant $g_{\rm A}$). This quantity is determined from the renormalised axial vector current $A_\mu^R = Z_A(1+b_A\,am_q)A_\mu$, where $am_q = (1/\kappa - 1/\kappa_c^{(S)})/2$. Z_A is known non-perturbatively [3], for b_A we use a tadpole improved one-loop perturbation theory result.

We have fitted our lattice results to an expression from ChEFT based on the SSE formalism. Using this formalism both the quark mass dependence [4] and the finite volume dependence [5] have been calculated. Since our results for different lattice spacings do not exhibit clear discretization effects we combine all our results where $m_{\rm PS} \leq 450\,{\rm MeV}$. The fit range has been chosen such that stable fits are obtained. Our data is not sufficiently precise to determine all parameters. We therefore fix a few parameters to their phenomenological value and keep only $g_{\rm A}$ in the chiral limit, the leading $\Delta\Delta$-coupling g_1 and the SSE coupling term $B_9^r(\lambda)$ as free fit parameters. The resulting fit and the lattice data are shown in Fig. 2a.

In our fit we only included results for the largest lattice at a given set of bare parameters. For some data sets we have results for different volumes. We thus can compute the relative shift

$$\delta_{g_{\rm A}}(L) = \frac{g_{\rm A}(L) - g_{\rm A}(\infty)}{g_{\rm A}(\infty)} \tag{3.1}$$

both from the fit as well as from the lattice data taking the results on the largest lattice as approximation of $g_{\rm A}(\infty)$. In Fig. 2b we compare the relative shift for different values of the quark mass with

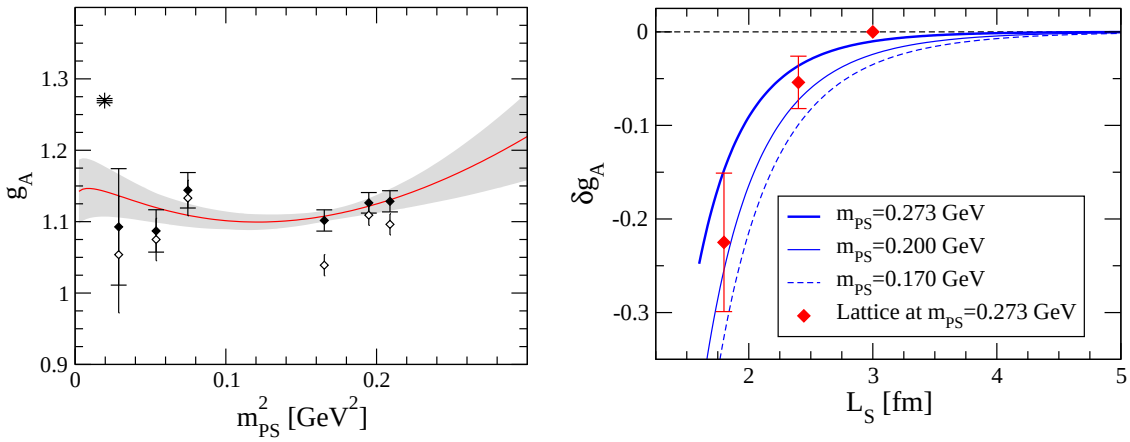

(a) (b)

Figure 2: The left panel shows g_A as a function of m_{PS}^2. The open and filled diamonds show the lattice results before and after correction of finite size effects, respectively. The star indicates the experimental result. The line shows a fit to the data as described in the text. The right panel shows the relative finite size effects determined on the lattice (symbols) and obtained from a fit to an expression from ChEFT.

our lattice results at $m_{PS} \simeq 270\,\text{MeV}$. The shift predicted from ChEFT only slightly underestimates the relative shift computed on the lattice.

Also after correcting for finite size effects we observe a significant difference to the experimental value. It is interesting to notice that a much better agreement with the experimental value is observed for the ratio g_A/f_{PS} (see Fig. 3a). In this ratio the renormalization constant Z_A drops out.

In Fig. 3b we show our results for the nucleon tensor charge $\langle 1 \rangle_{\delta q} = g_T$. We observe only a very mild quark mass dependence and the data reveals no systematic discretization effects. This quantity is not well known experimentally. Our values are larger than the phenomenological results presented in [6].

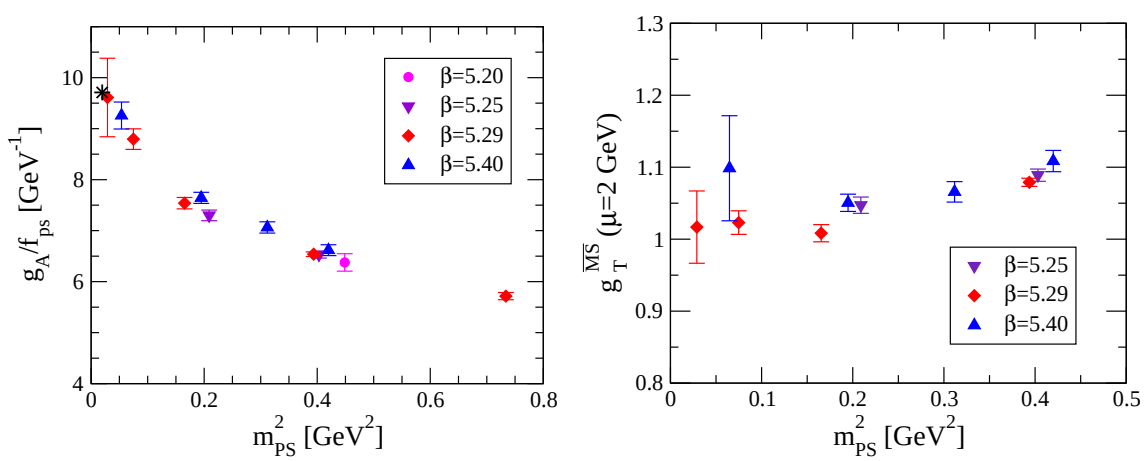

(a) (b)

Figure 3: The left panel shows g_A/f_{PS} as a function of m_{PS}^2. The right panel shows our results for $g_T^{\overline{MS}}$ at a scale $\mu = 2\,\text{GeV}$.

4. $n = 2$ moments of PDFs

The lowest moment of the unpolarized PDF $\langle x \rangle_q = v_2$ corresponds to the momentum fraction carried by the quarks in the nucleon. Lattice results from different collaborations tend to be significantly larger than the phenomenological value. Fig. 4a and 4b show our most recent results for the iso-vector and iso-scalar channel. In the latter case disconnected contributions have been ignored.

Also shown are the results from a fit to results utilizing methods of covariant Baryon Chiral Perturbation Theory (BChPT) [7]. Fits have been performed with most parameters fixed to phenomenologically known values. The iso-vector (iso-scalar) channel data is fitted with only 2 free parameters: v_2 in the chiral limit and the coupling c_8 (c_9). Near the physical light quark masses, BChPT predicts v_2 to become larger when the quark mass becomes heavier. In our data for $m_{\rm PS} \lesssim 250\,$MeV we do not see any indication for a bending down when approaching the physical pion mass. It thus does not seem that a lack of results at sufficiently small quark masses could explain the large discrepancy between the phenomenological value and the lattice results. There are some indications that part of the discrepancy can be explained by excited state contamination [8].

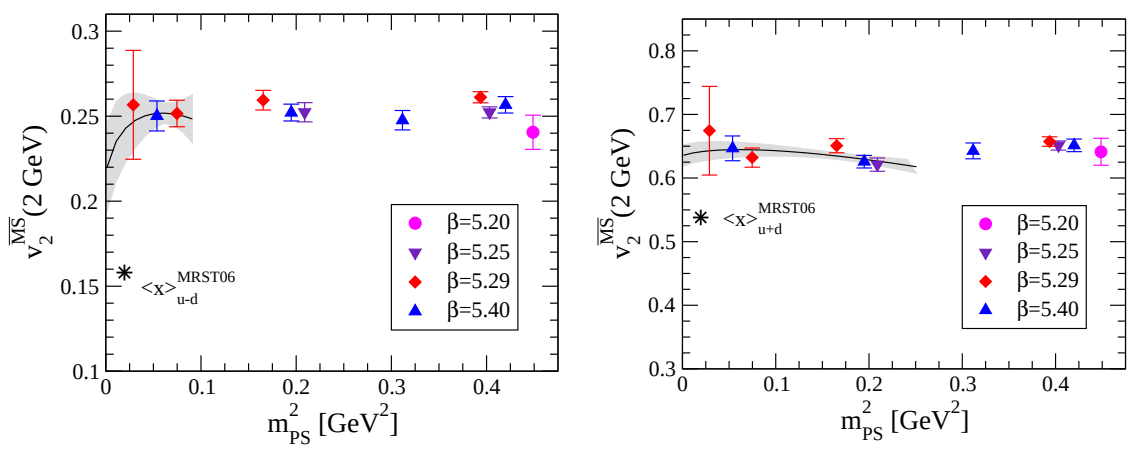

(a) (b)

Figure 4: The left and right panel show results for the second moment of the iso-vector and iso-scalar unpolarized PDFs, respectively, as a function of $m_{\rm PS}^2$. The solid lines show the fits to an expression from ChEFT.

In Fig. 5a the results for the second moment of the polarized PDF $\langle x \rangle_{\Delta q} = a_1$ is shown. Discretization effects again seem to be absent in data. From a comparison of the results for different volumes it seems that also finite size effects are small. Results from Heavy Baryon Chiral Perturbation Theory (HBChPT) [9] lead to the following expression:

$$a_1^{(u-d)}(m_{\rm PS}) = C\left[1 - \frac{4g_{\rm A}^2+1}{2(4\pi f_{\rm PS})^2} m_{\rm PS}^2 \ln\left(\frac{m_{\rm PS}^2}{\mu^2}\right)\right] + \cdots \tag{4.1}$$

In Fig. 5a we plot this expression using $\mu = m_{\rm N}$ and C chosen such that it matches the phenomenological value. The bending down which we observe in our data for $m_{\rm PS} \lesssim 0.5\,$MeV is much less than one would expect from this HBChPT result.

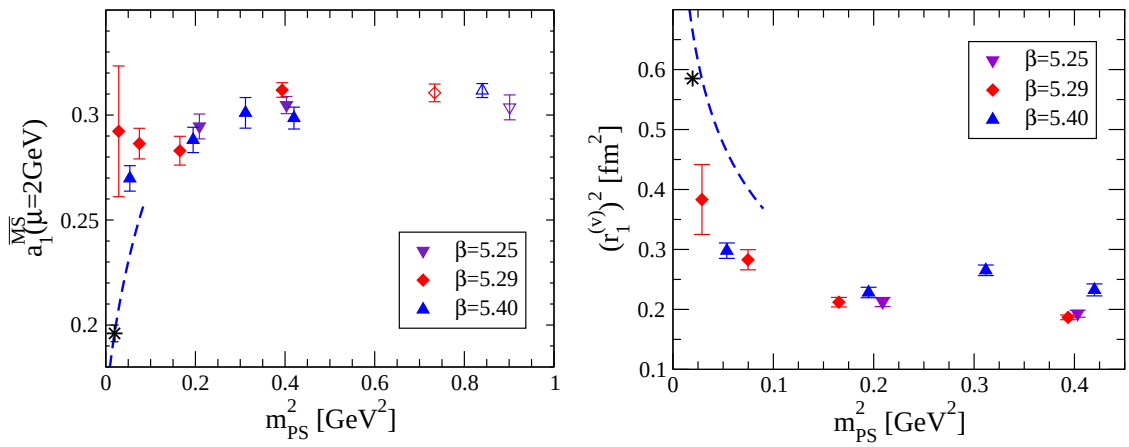

(a) (b)

Figure 5: The left panel shows the results for the second of the polarized PDFs as a function of $m_{\rm PS}^2$. In the right panel the results for the Dirac form factor radius r_1 are plotted. The dashed lines show results from ChEFT as described in the text.

5. Electromagnetic form factors

To compute the electromagnetic form factors one makes use of the standard decomposition of the nucleon electromagnetic matrix elements $\langle p',s'|V_\mu|p,s\rangle = \overline{u}\left[\gamma_\mu F_1(Q^2) + \frac{\sigma_{\mu\nu}q_\nu}{2m_{\rm N}}F_2(Q^2)\right]u$, (in Euclidian space) where we use the local vector current V_μ. p (s) and p' (s') denote initial and final momenta (spins), $q = p' - p$ the momentum transfer (with $Q^2 = -q^2$). To calculate form factor radii and the anomalous magnetic we have to parametrize the lattice results. Here we use the ansatz

$$F_i(Q^2) = \frac{F_i(0)}{\left[1 + \frac{Q^2}{pm_i^2}\right]^p} \tag{5.1}$$

with $p = 2$ and $p = 3$ for the Dirac and Pauli form factors F_1 and F_2, respectively. Our data is not sufficiently precise to favour a particular parametrization (see [10] for another parametrization).

From fits to Eq. (5.1) we determine the form factor radii r_1 and r_2 as well as the anomalous magnetic moment κ. The quark mass dependence of these quantities has been calculated using the SSE formalism [11]. For r_1 the parameters are known and we therefore restrict ourselves to a comparison of the SSE result and the lattice data (see Fig. 5b). While for $m_{\rm PS} \gtrsim 300\,$MeV the lattice results are significantly smaller than the phenomenological value, towards smaller quark masses we observe an increase of the radius. This is consistent with predictions from ChEFT. For r_2 and κ we find a similar behaviour. Since there are no phenomenological estimates for all parameters of the SSE expressions we perform a combined fit. The results are plotted in 6a and 6b.

6. Summary and outlook

We have presented an update of QCDSF results on the lowest moments of unpolarized, polarized and tensor PDFs as well as the electromagnetic form factors. Some of our results at light quark masses with $m_{\rm PS} \lesssim 300\,$MeV confirm the expectations from ChEFT that light quark mass effects are significant. However, this possibly does not explain all of the observed discrepancies from phenomenological values.

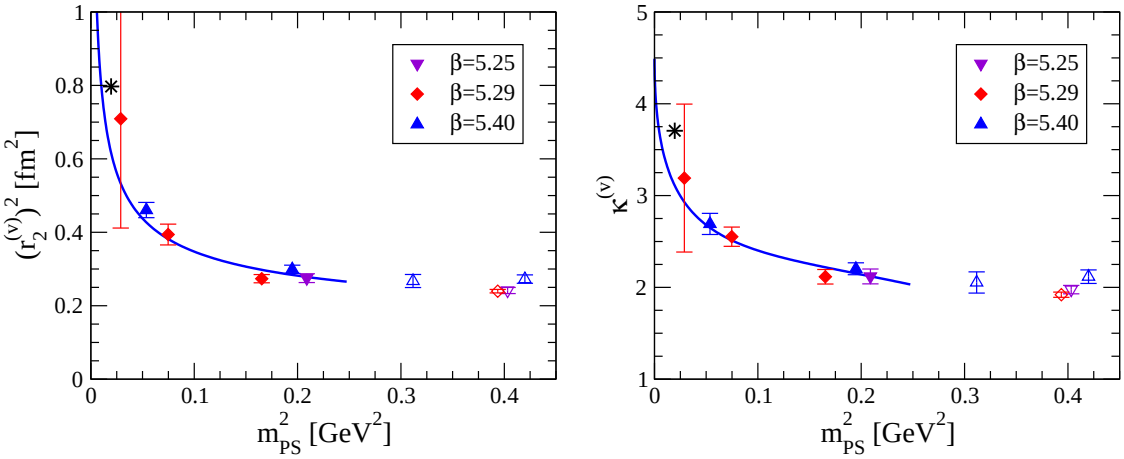

(a) (b)

Figure 6: The left panel and right panel shows the results for the Pauli radius r_2 and the anomalous magnetic moment κ. The solid lines show fits to an expression from ChEFT.

Acknowledgements

The numerical calculations have been performed on the APEmille and apeNEXT systems at NIC/DESY (Zeuthen), the BlueGene/P at NIC/JSC (Jülich), the BlueGene/L at EPCC (Edinburgh), the Dell PC-cluster at DESY (Zeuthen), the QPACE systems [12] of the SFB TR-55, the SGI Altix and ICE systems at LRZ (Munich) and HLRN (Berlin/Hannover). This work was supported in part by the DFG (SFB TR-55) and by the European Union (grants 238353, ITN STRONGnet and 227431, HadronPhysics2, and 256594).

References

[1] Y. Nakamura and H. Stüben, `PoS(LATTICE 2010)040`.

[2] A. Nobile, `PoS(LATTICE 2010)034`.

[3] M. Göckeler et al. [QCDSF Collaboration], `arXiv:1003.5756 [hep-lat]`.

[4] V. Bernard et al., Nucl. Phys. A635, 121 (1998); A642, 563(E) (1998). T.R. Hemmert, M. Procura, and W. Weise, Phys. Rev. D 68, 075009 (2003).

[5] A. Ali Khan et al. [QCDSF Collaboration], Phys. Rev. D 74 (2006) 094508.

[6] M. Anselmino et al., Nucl. Phys. Proc. Suppl. **191** (2009) 98-107.

[7] M. Dorati, T. A. Gail and T. R. Hemmert, Nucl. Phys. A **798** (2008) 96.

[8] M. Göckeler et al., in preparation.

[9] D. Arndt and M.J. Savage, Nucl. Phys. A697, 429 (2002); J.W. Chen and X. Ji, Phys. Lett. B 523, 107 (2001); W. Detmold, W. Melnitchouk and A. W. Thomas, Phys. Rev. D **66** (2002) 054501.

[10] M. Göckeler et al. [QCDSF Collaboration], `PoS(LATTICE 2007)161`.

[11] T. R. Hemmert and W. Weise, Eur. Phys. J. A **15** (2002) 487 [arXiv:hep-lat/0204005]; M. Göckeler et al. [QCDSF Collaboration], Phys. Rev. D **71** (2005) 034508 [arXiv:hep-lat/0303019].

[12] H. Baier et al., `PoS(LATTICE 2009)001`.